

Overcoming limitations of etalon spectrometers used for spectral metrology of DUV excimer light sources

Robert J. Rafac*, Cymer, Inc., 17075 Thornmint Ct., San Diego, CA 92127-1712

ABSTRACT

Etalon spectrometers often provide the practical means for providing pulse-resolved spectral metrology of line-narrowed excimer laser lithographic light sources because of their relative simplicity and physical robustness. A typical application uses the full-width at half-maximum intensity (FWHM) of an etalon fringe to infer the FWHM bandwidth of an unknown input spectrum. These devices are often used in a regime where the ratio of the width of the spectrometer impulse-response to the bandwidth of the source spectrum is close to (or greater than) unity. In this regime, the fringe width may have non-negligible sensitivity to details of the source spectral shape other than its FWHM, including asymmetry and spectral purity. This paper details this sensitivity and provides suggestions for techniques that can either suppress the effect or apply it to some advantage such as estimation of a spectral purity metric, *e.g.*, the 95%-enclosed energy width (E95%) of the source spectrum.

Keywords: Excimer laser, bandwidth, metrology, chromatic aberration, spectrometer

1. INTRODUCTION & MOTIVATION

The output spectrum of a line-narrowed excimer laser light source for DUV lithography is not generally constant in time. While stability has greatly improved with advances in technology, neither the bandwidth nor the functional form (shape) of the spectrum is perfectly fixed. The impact of spectral shape changes on lithographic performance is incompletely characterized; however, the influence of full-width at half-maximum (FWHM) and 95%-enclosed-energy (E95 or "spectral purity") illumination bandwidths on image contrast, log-slope, exposure latitude, *etc.* have already been found to be significant by other investigators^{1,2}. Dependence on the illuminating spectrum arises because optical material constraints at DUV wavelengths make some chromatic aberration unavoidable in projection lenses for KrF and ArF lithography. While chromatic effects can be minimized with a spectrally narrowed light source, even sub-picometer broadening of the illumination spectrum cannot be completely ignored³. The concern becomes more pressing as the industry moves to ever-higher numerical aperture and lower k_l . To guarantee that the aerial image properties are maintained within a given process window, it is therefore increasingly important to have trustworthy metrologic feedback from the light source reporting these spectral figures-of-merit with high accuracy and reliability. Further, in more advanced applications this information can actually be used to control the workings of the light source in some way, so as to stabilize the light source spectrum or otherwise modulate its bandwidth. In such scenarios, the enhanced spectral performance repeatability obtained means that generic optical-proximity (OPC) solutions can be imagined that remain effective and consistent over the system lifetime and/or population.

Commonly used bandwidth metrics such as FWHM and E95 are not always accurate measures of spectral shape, especially when either is considered alone. For example, an increase in the energy content of the far wings of the spectrum will increase the E95 while leaving the FWHM bandwidth unchanged. Other spectral shape changes leave the E95 constant while altering the FWHM, or may leave both these metrics constant while changing the center-of-energy of the spectrum, *etc.* We will show that these shape changes often go hand-in-hand with bandwidth changes, with significant consequences for the design of spectral metrology tools.

2. SPECTRAL SHAPE VARIATIONS OF DUV LIGHT SOURCES FOR MICROLITHOGRAPHY

Variations in spectral shape and bandwidth of ultra-narrow excimer laser light sources originate in a variety of physical mechanisms. Some of this variation is technically unavoidable, but the design of the light source is generally optimized

* Robert_Rafac@cymer.com, www.cymer.com

to minimize it. Even with engineering controls, large changes in spectral shape or bandwidth sometimes occur due to improper alignment, failure of optical components, or failure to manage important process parameters internal to the light source (*e.g.*, laser gas mixture). It is usually the job of an onboard spectral metrology package to correctly identify and accurately report the light source bandwidth so that it may be used as trustworthy input to the lithographic process control. To illustrate some spectral shape and bandwidth changes, a number of examples of variation seen in a Cymer XLA 100 ArF MOPA (Master-Oscillator/Power-Amplifier) light source measured with a high-resolution double-pass echelle grating spectrometer are shown in Fig. 1. This collection is not exhaustive, but is believed to be typical of a light source of the current generation. The data have been normalized to equal total energy for better comparison of the spectral energy distribution, and represent the integrated spectral content for an exposure of 200 laser pulses.

Example I demonstrates the effect of greatly enriching the fluorine concentration of the laser gas in the master-oscillator of a MOPA or the gain medium of a single-oscillator ArF light source. With the addition of extra fluorine to the gas mixture at constant total pressure, the bandwidth increases. In these measurements the E95 of the output spectrum increased by 18% as the fluorine was enriched to 13% above the initial concentration. However, the spectral FWHM was found to stay constant within the precision of the measurement for the same enrichment. This indicates a significant change in the functional form of the spectrum—not simply a rescaling of the wavelength axis. Such a large over-enrichment of the laser gas mix is not typical, but could be representative of a hypothetical failure mode of a light source's internal controls.

Example II illustrates the effect of an acoustic disturbance timed to pass through the electrode gap during laser oscillation. As evidenced by the fact that the wings of the spectrum remain fixed while the central peak of the spectrum flattens and widens, the shape of the spectral profile changes due to this effect. This shape change has features opposed to those of the previous example—in this case the FWHM bandwidth increased by 52% over the nominal value obtained away from the time-of-flight (TOF) resonance, while the E95 only rose 8% beyond the nominal value. The size of the TOF resonance effect can be greatly reduced with careful discharge chamber designs, but is present to some degree in all high-repetition rate systems.

Example III illustrates a shape change due to a very large static error in the relative timing of the gain onset in the two chambers of a MOPA light source. This phenomenon arises because the spectral shape and bandwidth of the MO output is time-dependent within a pulse; this behavior is therefore unique to MOPA systems (MOPO architectures have a further spectral complication due to gain competition between the injected and free-running modes of the power oscillator). In normal operation, the delay between firing of the two chambers is chosen to be that time τ_0 corresponding to the peak of MOPA-system electrical-to-optical conversion efficiency. In this measurement of shape versus time delay, the bandwidth decreased by about 10% in FWHM and 25% in E95 when the delay was increased to τ_0+10 ns. When the delay was shortened to τ_0-10 ns, the bandwidth was seen to increase by approximately the same amount. Changing this delay can be used to control the bandwidth in a MOPA configuration, but such large offsets from the efficiency peak introduce trade-offs against controlling other properties of the laser output.

The final example IV shows the response of the laser spectrum to an exaggerated wavefront curvature inside the resonator of a grating-narrowed laser oscillator (MO or single-chamber oscillator). In this experiment the surface figure of a reflecting optic inside the line-narrowing subsystem was artificially distorted by application of mechanical force to simulate the effects of a defective component inside the laser cavity. The effect on spectral shape was quite profound, as can be seen in the figure. This is a second example where the FWHM was altered very little by the shape change, but the E95 changed by nearly a third. The symmetry of the spectrum was also destroyed by this perturbation. This kind of variation is not normal for a well-designed light source, but has been observed to become manifest with a defective or failing optic due to excessive thermal loading, *etc.* These four cover the dominant types of spectral shape variation seen in Cymer, Inc. research and development.

3. BANDWIDTH MEASUREMENT AND ESTIMATION TECHNIQUES FOR DUV LIGHT SOURCES

Because of the concomitant variation of spectral shape and bandwidth, development of accurate and optomechanically robust spectral metrology on a per-pulse basis for a high repetition-rate excimer laser source is more technically

challenging than may heretofore have been appreciated. For future-generation light sources, an ideal spectral metrology solution would have the following five features:

- i. **Very high spectroscopic resolution.** This can be recast more rigorously by requiring that the impulse response (instrument function) of the spectrometer have a bandwidth many times smaller than that of the light source spectrum.
- ii. **Wide inspection range in wavelength (λ) space.** It has been argued⁴ that even small changes in the far wings of the illumination spectrum significantly impact the aerial image properties; this requirement is similarly necessary for direct computation of E95.
- iii. **Accurate and robust method for disentangling (deconvolving) the bandwidth of the source spectrum from the instrument function of the spectrometer,** which in general is non-negligible. This could either be a direct deconvolution using an independent measurement of the instrument function, or some sort of mathematical or semi-empirical model that obtains a similar result or estimate.
- iv. **High signal-to-noise ratio (SNR) for a single-pulse measurement.** This is required for per-pulse assessment of spectral quality and lithographic process judgment.
- v. **Optical and mechanical simplicity and robustness**—necessary for stability of calibration, repeatability of measurement, and long-life in a production environment.

It is difficult if not impossible to simultaneously satisfy all of these requirements with current technology. Multi-pass grating spectrometers (Fig. 2) can provide excellent spectroscopic resolution, wide inspection ranges, and ability to deconvolve the influence of the instrument function using Fourier or other methods. On the downside, grating spectrometers are bulky, fragile, generally require moving parts for tuning, and can be hard to maintain. Because of their low acceptance, high-resolution grating spectrometers also require long exposures for adequate SNR, rendering them impractical for per-pulse reporting of spectrum quality. They are also expensive, commanding prices that may reach a significant fraction of the total outlay for a high-performance light source. Grating spectrometers are indispensable tools for system qualification and in research roles where very fine details of spectral shape and out-of-band energy distribution must be accurately characterized in terms of spectral purity, line asymmetry, *etc.* They are not generally practical, however, for onboard real-time measurement in lithography production applications.

Fabry-Perot etalon spectrometers (Fig. 3) provide an alternative solution. They are optically simple and can be made mechanically robust with no moving parts. The lack of necessity for a slit means that for a given input, a large irradiance can be obtained in the detector plane in spite of poor beam quality. Because of this a plane-mirror etalon can capture useful spectral information from a single short pulse of illumination by utilizing the angular discrimination between transmitted beams at different wavelengths.

To compete with grating spectrometers purely on the basis of spectroscopic resolution and inspection interval, long free spectral range (FSR), high transmission, and high-finesse (\mathfrak{F}) etalons are required. A commercial double-pass echelle grating spectrometer for use in the DUV might achieve a fixed inspection range of 15 pm and an instrument function of 50 fm FWHM bandpass when operating in high order. To match this performance with an etalon spectrometer, an FSR \approx 15 pm and a finesse of $\mathfrak{F} \approx 300$ would be required. While this kind of performance may be surpassed for longer wavelengths, it is not practical in the DUV where surface figure (parallelism, flatness, roughness) and mirror coating limitations typically limit the total finesse to $\mathfrak{F} < 50$. The finesse loss due to geometric imperfection can be reduced by using a mode degenerate spherical-confocal etalon. In this arrangement the focusing effect of the spherical mirrors results in a mode diameter that is small on the mirror surface, suppressing the influence of geometric imperfections. Unfortunately, in this configuration the inter-mirror optical path length must be scanned for spectral analysis, making analysis of isolated short pulses or few-pulse bursts impossible. Further, for a given spacing the FSR is halved using this method, and the mode-matching requirement means that the insertion loss may be prohibitively high for beams of poor quality. Therefore, the confocal arrangement discards many of the special advantages of the etalon spectrometer when trying to obtain grating spectrometer-like performance. A similar conclusion obtains for other schemes that obtain high spectroscopic resolution and large inspection ranges with series arrangements of multiple etalons.

In spite of their limitations, air-spaced plane-etalon spectrometers are still often the best choice for numerous spectral measurement tasks. While not offering the largest inspection ranges or resolving powers in the DUV, reasonable

compromises can be reached in these areas while retaining their superior single-short-pulse SNRs and adaptability to manufacturing applications that require physical robustness and reliability. For spectral monitoring of lithographic tool illumination, plane etalons with FSRs from 2 to 40 pm attaining finesse values from 20-50 are commonly employed. This means that these devices are used in a regime where the ratio of the FWHM bandpass of the spectrometer instrument function to the bandwidth of the source spectrum is close to or greater than unity. In this regime, the etalon FWHM fringe width may have non-negligible sensitivity to details of the source spectral shape other than its FWHM, including spectral purity. It was demonstrated in §2 that the spectral shape of DUV light sources can vary significantly, particularly in cases of failing components or controls. These shape changes may “hide” beneath the instrument function of the spectrometer and influence its output. Therefore, a very special emphasis must be placed on the third requirement listed above—namely, that the method used to estimate the bandwidth of the source spectrum from the etalon fringe measurement be dependable and accurate.

4. IMPACT OF SPECTRAL SHAPE ON ESTIMATION OF SOURCE BANDWIDTH

A number of techniques can be applied to recover the complete source spectrum or source bandwidth from a spectrometer measurement. Recall that the signal output $O(\lambda)$ by a spectrometer is the convolution of the source spectrum $S(\lambda)$ and the instrument function of the spectrometer $I(\lambda)$:

$$O(\lambda) = \int_{-\infty}^{\infty} S(\Lambda)I(\lambda - \Lambda)d\Lambda \quad (1)$$

Three methods are commonly employed to determine the bandwidth of a source spectrum $S(\lambda)$ given the spectrometer signal $O(\lambda)$. The most complete is a full deconvolution of the output signal $O(\lambda)$. Given $O(\lambda)$ and an independent determination of $I(\lambda)$, a solution to Equation 1 can be found using Fourier or other methods. This can be a challenging task, because in general there are many source spectra $S(\lambda)$ that convolve with $I(\lambda)$ to give the same output signal $O(\lambda)$. Usually special efforts must be made to deal with noise in the measurements and zeros in $I(\lambda)$, and for a fine-grained spectrum this process can take a considerable amount of processing time. For these and other reasons, this method is generally not well suited for monitoring of the bandwidth of a light source spectrum on a per-pulse basis in high-repetition rate applications. This method is still preferred when using high-resolution grating spectrometer measurements for basic research or in light-source manufacturing test environments, where very detailed knowledge of the full spectrum is required.

A second technique appeals to mathematical arguments made on the basis of analytic approximations of the source spectrum and instrument function. For example, in the cases where the spectral densities $S(\lambda)$ and $I(\lambda)$ are both perfectly Lorentzian or both perfectly Gaussian in distribution, the FWHM and E95 bandwidths of the source spectrum $S(\lambda)$ are very simply related to the “bandwidths” of $O(\lambda)$ and $I(\lambda)$. Consider a Lorentzian source spectrum with FWHM bandwidth Γ_S and Lorentzian instrument function with FWHM bandpass Γ_I . Then

$$S(\lambda) = \frac{1}{\pi} \frac{\Gamma_S/2}{(\lambda - \lambda_0)^2 + (\Gamma_S/2)^2}, \quad I(\lambda) = \frac{1}{\pi} \frac{\Gamma_I/2}{(\lambda - \lambda_0)^2 + (\Gamma_I/2)^2} \quad (2)$$

$$O(\lambda) = \int_{-\infty}^{\infty} S(\Lambda)I(\lambda - \Lambda) = \frac{1}{\pi} \frac{(\Gamma_S + \Gamma_I)/2}{(\lambda - \lambda_0)^2 + ((\Gamma_S + \Gamma_I)/2)^2} \Rightarrow \Gamma_S = \Gamma_O - \Gamma_I.$$

In this case the FWHM bandwidth Γ_S of $S(\lambda)$ is found just by subtraction of the constant Γ_I from the output signal bandwidth Γ_O . The E95 could be handled similarly, because

$$E \left[\frac{1}{\pi} \frac{\Gamma/2}{(\lambda - \lambda_0)^2 + (\Gamma/2)^2} \right] = \Gamma \tan(0.95 \frac{\pi}{2}) \approx 12.71\Gamma, \quad (3)$$

where $E[\dots]$ denotes the E95 bandwidth of the bracketed spectral distribution.

A third and widely used method for obtaining the light source bandwidth without full deconvolution begins with Equations 2 and 3 as a first approximation, but modifies the form or adds additional corrective terms to reduce the systematic error that results from imperfect assumptions about the shape of the source spectrum and/or instrument

function. It is therefore semi-empirical in character and requires calibration against a trusted measurement. In a typical scenario the light source is run through some series of operating modes or conditions that cause its bandwidth to vary. The source FWHM bandwidth Γ_S is carefully determined during this test using an external high-resolution grating spectrometer and Fourier deconvolution (or by some other means). At the same time, the output of the metrology system undergoing calibration is recorded—this output is usually the fringe width w of an etalon spectrometer contained inside the light source. With this data in hand, the source bandwidth Γ_S can be estimated by devising a relation $\Gamma_S \approx f(w)$. The best choice for the semi-empirical model f can be made from inspection of the data and/or by recourse to mathematical reasoning like that in the preceding paragraph. It is very important that during the calibration process the source be made to range over the entire range of accessible shapes and bandwidths, or the model will be at risk for error.

Let us look at some semi-empirical models in more detail. The simplest choice of model for FWHM bandwidth estimation is the subtraction of an experimentally determined constant offset:

$$\Gamma_S \approx f(w) = w - \delta \quad (4)$$

This model is mathematically exact when both the light source spectrum and the instrument function of the spectrometer are purely Lorentzian (Equation 2). Etalon spectrometers do have instrument functions $I(\lambda)$ that are very nearly Lorentzian, but as suggested in §2 the spectrum $S(\lambda)$ of the DUV light source is in general not well approximated by either a Gaussian or Lorentzian distribution, and in fact can be quite difficult to parameterize. The simple fact that the ratio E95/FWHM is not constant for the spectra shown in Fig. 1 provides a straightforward indication that Gaussian or Lorentzian assumptions are inadequate, because this ratio is constant for these analytic forms (Equation 3, *etc.*). Therefore one finds that the constant offset model (4) will give an imperfect estimate of the source bandwidth Γ_S , subject to a systematic error dependent on the detailed spectral shape. To illustrate this point, consider a hypothetical light source the spectrum $S_V(\lambda)$ that is shaped very nearly like a Voigt profile. A Voigt profile is a convolution of Lorentzian and Gaussian distributions having equal energy content:

$$S_V(\lambda) = \int_{-\infty}^{\infty} d\lambda' \left(\frac{1}{\pi} \frac{\Gamma_S/2}{\lambda'^2 + (\Gamma_S/2)^2} \cdot \frac{1}{\sigma\sqrt{2\pi}} \exp\left[-\frac{1}{2}\left(\frac{\lambda - \lambda'}{\sigma}\right)^2\right] \right). \quad (5)$$

This source spectral shape is completely characterized by two parameters, which are the FWHMs Γ_L and $\Gamma_G = 2\sigma\sqrt{-2\ln(1/2)} \approx 2.35\sigma$ of the Lorentzian and Gaussian components. The output $O_V(\lambda)$ of an etalon spectrometer illuminated by this source is well-approximated by the convolution of $S_V(\lambda)$ with a purely Lorentzian instrument response $I(\lambda)$, where the FWHM bandpass γ of this Lorentzian is given by the ratio of the etalon FSR to its finesse \mathfrak{S} :

$$O_V(\lambda) = \int_{-\infty}^{\infty} d\Lambda \left(\frac{1}{\pi} \frac{\gamma/2}{\Lambda^2 + (\gamma/2)^2} \cdot S_V(\lambda - \Lambda) \right); \quad \gamma = \frac{\text{FSR}}{\mathfrak{S}}. \quad (6)$$

Fig. 4 plots the difference between the FWHM of the calculated etalon spectrometer output fringe $O_V(\lambda)$ and the FWHM of the source spectrum $S_V(\lambda)$ in units of γ as a function of the two independent shape parameters Γ_L/γ and Γ_G/γ . As $\Gamma_G \rightarrow 0$, the difference δ between the etalon fringe FWHM and the FWHM of the source spectrum approaches a limiting value of γ as expected—this is the condition described by Equation 2. But as the width of the Gaussian component increases, δ gets smaller and the constant-offset model of Equation 3 fails to give an accurate estimate of the source bandwidth. This model is somewhat artificial, but illustrates the variation between limiting cases of Lorentzian and Gaussian light sources clearly.

Performance of the constant-offset model may be improved by extending it to a point-slope model

$$E_S \text{ or } \Gamma_S \approx f(w) = Aw - B. \quad (7)$$

The point-slope model works well for the hypothetical Voigt spectral distribution $S_V(\lambda)$ only if the parameters Γ_L and Γ_G are constrained in their variation; for example, if there is a smooth monotonic relationship between them and the overall bandwidth variation of $S_V(\lambda)$ does not cover too wide a range. However, if the spectral shape is poorly constrained the point-slope model fails. In the case of FWHM estimation, it is worth a reminder that the performance of these simple models improves greatly when the FWHM bandpass of the instrument function $I(\lambda)$ is made very small. As discussed in §3, this is however difficult or impossible to achieve for plane etalon assemblies of even moderate FSR in the DUV.

5. ROBUST METHODS FOR ESTIMATION OF BANDWIDTH USING ETALON SPECTROMETERS

The preceding discussion casts some doubt on the applicability of available etalon spectrometers to the accurate and reliable bandwidth estimation of line-narrowed DUV sources. However, recent investigations at Cymer, Inc. indicate that with a clear understanding of the limitations of the technique, robust semi-empirical FWHM and E95 bandwidth estimation using relatively wide bandpass etalon measurements may still be obtained. We are studying a number of methods for estimating the bandwidth of ArF excimer light source spectra using the width of etalon fringes as input. By construction, these techniques are designed to suppress or actively correct systematic errors that arise due to spectral shape change. Most of the methods under investigation rely on the following three simple observations:

- The wider the FWHM bandpass $\gamma = \text{FSR}/\mathfrak{S}$ of the etalon, the more the fringe FWHM w is influenced by energy in the wings of the source spectral distribution (and hence its E95).
- If the full-width at X% of peak intensity (FWX%) of the fringe is measured, as $X \rightarrow 100\%$ the full-width depends mostly on the energy content near the center of the source spectral line. As $X \rightarrow 0\%$, the full-width depends more on the energy content in the wings of the source spectrum.
- The space of bandwidths and spectral shapes accessible to a single-oscillator or MOPA light source is constrained to a limited range, even in cases of pathological operation or failure of internal components.

With these points in mind, we have found in tabletop experiments that it is possible to “optimize” the choice of etalon bandpass γ , the fringe measurement threshold, and the bandwidth estimator model to obtain an accurate prediction of the source FWHM or E95 bandwidth that is relatively immune to limited variations in the source spectral shape.

In the course of our experiments we have collected large spectral sample populations and have studied the response of real and simulated etalon spectrometers. We find that a spectrometer of FWHM instrumental bandpass γ illuminated by these spectra responds with a fringe width w that is relatively well-modeled by the equation

$$w(X\%, \gamma) \approx A(X\%, \gamma)\Gamma_S + B(X\%, \gamma)E_S + C(X\%, \gamma), \quad (8)$$

where A , B , and C are constants that depend on the spectrometer instrument function and the fraction of intensity $X\%$ at which the full-width of the fringe is measured, and Γ_S , E_S are the FWHM and E95 of the source spectrum $S(\lambda)$, respectively. Equation 8 is a further generalization of the models discussed in §4, rearranged to express the dependence of the fringe width on the source spectrum instead of vice-versa. When the ratio $E_S/\Gamma_S = \text{constant}$ or $E_S = \text{constant}$ the point-slope model obtains, and when either of these conditions hold with $A \approx 1$, the constant-offset model obtains. The coefficients of (8) can be determined by computer simulation or calibration against a trusted standard. In practice, it is helpful to use simulations as a guide in choosing the parameters X , γ and the functional form of the estimator model to obtain the desired sensitivity. The suitability of Equation 8 can be judged for a given population of spectral shapes by plotting the fringe width versus the E95 and FWHM of the source spectrum. The model can be validated by plots such as that shown in Fig. 5, where the ratio E_S/Γ_S is not constant over the population but the data still lie close to a plane in (Γ_S, E_S, w) -space. This model is not perfect, particularly because A , B , and C still depend to some degree on the class of spectral shapes measured, but appears to hold for a useful range of (Γ_S, E_S, γ) values. Note that a plane also obtains when $E_S/\Gamma_S = \text{constant}$, so it is important to verify the behavior using a spectral sample that has significant variation in this ratio.

For experimentally determined spectral shapes of the kind described in §2, we find that best fits of (8) to the data yield $A \approx B$ when $\gamma \approx E_S$ and $X = 50\%$. If $\gamma \approx E_S/2 \approx \Gamma_S$ and $X = 50\%$, we find that $A \approx 3.5B$. This quantifies somewhat the observation that as the etalon instrument function narrows, the fringe width more linearly tracks the source spectral FWHM in spite of shape changes. This behavior has significant implications for spectrometer design. If a point-slope model is used to estimate the FWHM bandwidth of a source spectrum from the FWHM of an etalon fringe, a significant amount of E95 “bleeds through” the instrument function (see Fig. 6) into the fringe width if γ is too wide. This happens because convolution with the instrument function pulls some energy from the wings of the source spectrum into the core of the etalon fringe. If the FWHM (~core) and E95 (~wings) of the source spectrum vary independently as they do in the examples of §2, a systematic error will appear in the estimate of the source FWHM (Fig. 7).

In designing an etalon spectrometer, the available choices of $\gamma = \text{FSR}/\mathfrak{S}$ are highly constrained by the availability of high-quality reflective coatings, low-loss/high-flatness substrates, and cavity spacers with very low wedge angles—so the optimal choices are not always available. The model (8) suggests that some remedy may still be found by adjusting the threshold parameter X , however. The results of a simulation plotted in Fig. 8 illustrate the effect of increasing the measurement threshold X from 25% to 50% to 75% of the fringe peak intensity on the error in estimating the FWHM bandwidth of a large population of source spectra with shape variation using a point-slope model and $\gamma \approx \Gamma_s$. The improvement found with increasing X can be attributed to a reduction in the sensitivity of the width measured at higher thresholds to variation in the balance of energy between the core and wings of the source spectrum. This is because the process of convolution with $I_\gamma(\lambda)$ allows less energy from the wings of the source spectrum to contribute to the FW75% compared to the FW25% for this choice of γ .

6. APPLICATION TO E95 METROLOGY

The fact that source spectral E95 variations at constant FWHM can be clearly discerned in the FWX% of an etalon spectrometer fringe (Fig. 6 and 7) means that it is sometimes possible to estimate the E95 of a light source spectrum without recourse to deconvolution and full integral treatment of the data. In terms of the model (8), for application of a plane-etalon spectrometer to FWHM estimation it is often sufficient to make γ as small as practical and increase X to the maximum level permitted by the angular resolution of the fringe detector. In such a case, $A/B > 5$ and the sensitivity to shape change will be small enough to be acceptable. For E95 estimation, however, the situation is more challenging because it is difficult to construct a scenario where A/B is much less than unity while still satisfying constraints that originate in other aspects of the spectrometer design (detector resolution and noise, *etc.*)

In our research we examined the usefulness of etalon spectrometers for application to E95 metrology by examining the behavior of the FW35% and FW75% fringe widths of an experimental spectrometer with $\gamma = 0.65 \text{ pm} \approx \text{Max}\{E_s\}$. This γ was chosen because it gives acceptable sensitivity to the energy content in the wings of the source spectrum without excessively compromising other performance aspects. In the experiments, a Cymer XLA 100 prototype was run over a wide range of conditions within and beyond its normal operating envelope so as to generate significant variations in bandwidth and spectral shape of its output (corresponding to conditions and variations of the types I-III of §2). The light from this source was homogenized and used to illuminate both a high-resolution double-pass echelle grating spectrometer and the experimental etalon spectrometer simultaneously. The grating spectrometer output was deconvolved using Fourier methods and the corresponding E95 bandwidths were computed. The etalon fringe patterns obtained during the grating spectrometer exposure were analyzed and the fringe FW35% and FW75% values reported. The results are presented in Fig. 9 as a plot of the fringe width at the two intensity thresholds versus the E95 of the deconvolved source spectrum recorded by the grating spectrometer. Viewed from a point-slope perspective

$$E_s \approx m \cdot w(X\%, \gamma) + b, \quad (9)$$

the fringe width follows the source E95 bandwidth change due to MOPA timing offset and fluorine enrichment with one slope m , but responds with a completely different slope $m \neq m$ against source E95 change due to chamber acoustic phenomena—a consequence of the different types of concomitant variation in bandwidth and spectral shape associated with different physical processes within the laser. The best-fit intercepts b also vary as a function of operating point. We concluded from this and other experiments that a full-width measurement at a single intensity threshold X is insufficient for robust E95 estimation in the presence of spectral shape variation.

Because the single-threshold approach was inadequate, we considered some other strategies that follow from the fringe width model (8). In one technique, two etalon spectrometers are designed so as to obtain sufficiently different coefficients A , B , C for each. These spectrometers may be operated simultaneously and in parallel to obtain two different fringe widths; armed with these fringe widths and the set of six coefficients, the system of two equations may be solved for the unknown source FWHM and E95. This method has the cost and complexity disadvantage of requiring two separate etalon spectrometers working in parallel, but simulations we performed indicate it can report good estimates of both the FWHM and E95 of the source if the coefficients are chosen properly and certain detection constraints can be satisfied.

A method that provides a robust E95 estimate of the source spectrum while using only a single etalon applies (8) in a different way. In this approach, the etalon bandpass γ is fixed by the finesse and choice of FSR, but the values of the coefficients A , B , and C can still be changed in a significant way by altering the intensity threshold X at which the fringe width measurement is performed. For two sufficiently different choices of X , a plane equation is again obtained. To test this idea, we repeated our experiments with the E95 estimator model altered to use two intensity thresholds. In this set of measurements, we took as our model

$$E_s \approx K \cdot w(35\%, \gamma) + L \cdot w(75\%, \gamma) + M, \quad (10)$$

where K , L , M are calibration constants determined by the best fit of the source spectral E95 (measured with the grating spectrometer) to the model. The source E95 estimation accuracy over a wide range of spectral shape variation is significantly improved by using (10), as can be seen by the experimental results plotted in Fig. 10. In accordance with the fringe model (8), we believe that the combination of the two FWX% terms partly “senses” independent changes of the source spectral energy distribution in the core and near wings of the spectral line. Equation 10 therefore corrects for the independent variation of FWHM and E95 to which the simple one-dimensional point-slope model is insensitive. Close inspection still reveals some residual systematic deviation, but the sigma of the error distribution for the given spectral population was reduced by about a factor of two when applying this new technique.

Other strategies are also under investigation at Cymer, Inc. One such method computes the $X\%$ enclosed-energy width (EX%) of the etalon spectrometer fringe and uses it as input to a point-slope or other model. This method also shows promise for improved estimation of source E95, but requires much more computation due to the integration required. It may have certain advantages, however, when it comes to latitude in etalon selection and other aspects of the spectrometer design. During preparation of this manuscript, a number of improved methods were still being evaluated for implementation in our next generation of light sources. We expect to choose the best-performing and most robust solution.

7. SUMMARY AND CONCLUSIONS

In spite of a variety of shortcomings, etalon spectrometers have distinct advantages for application to bandwidth metrology onboard the line-narrowed excimer light sources used in DUV lithography. These light sources exhibit dependence of the detailed shape or functional form of their output spectra on specific operating conditions. Such shape changes can introduce substantial systematic errors into the methods commonly used to estimate bandwidth, due to the non-negligible bandpass of the instrument function present in practical embodiments of these spectrometers. Fortunately, through application of a simple etalon fringe width model we have discovered some special methods that are less sensitive to these spectral shape variations. When used with care, these techniques can suppress errors related to spectral shape change by introducing or suppressing measurement sensitivity to the relative energy distribution between the core and near wings of the spectrum. Because of the sensitivity of the lithographic process to the illumination bandwidth, management of this source of systematic error is expected to be important to current and future applications—particularly those involving active control or stabilization of the source spectrum.

REFERENCES

1. “Contribution of polychromatic illumination to optical proximity effects in the context of Deep-UV lithography”, A. Kroyan, I. Lalovic, N. R. Farrar, *Proc. 21st Annual BACUS Symposium on Photomask Technology and Management*, G. T. Dao and B. J. Grenon (Eds.), Monterey CA, SPIE Vol. 4562, pp. 1112-1120, 2002.
2. “Understanding chromatic aberration impacts on lithographic imaging”, K. Lai, I. Lalovic, R. Fair, A. Kroyan, C. Proglor, N. R. Farrar, D. Ames, K. Ahmed, *J. Microlithography, Microfabrication and Microsystems*, Vol. 2, Issue 2, pp. 105-111, 2003.
3. “Modeling the effects of excimer laser bandwidth on lithographic performance” A. Kroyan, J. J. Bendik, O. Semprez, N. R. Farrar, C. G. Rowan and C. A. Mack, SPIE Vol. 4000, *Optical Microlithography XIII*, pp. 658-664, March 2000.
4. “Effects of 95% integral vs. FWHM bandwidth specifications on lithographic imaging”, A. Kroyan, I. Lalovic and N. R. Farrar, SPIE Vol. 4346, *Optical Microlithography XIV*, pp. 1244-1253, March 2001.

FIGURES

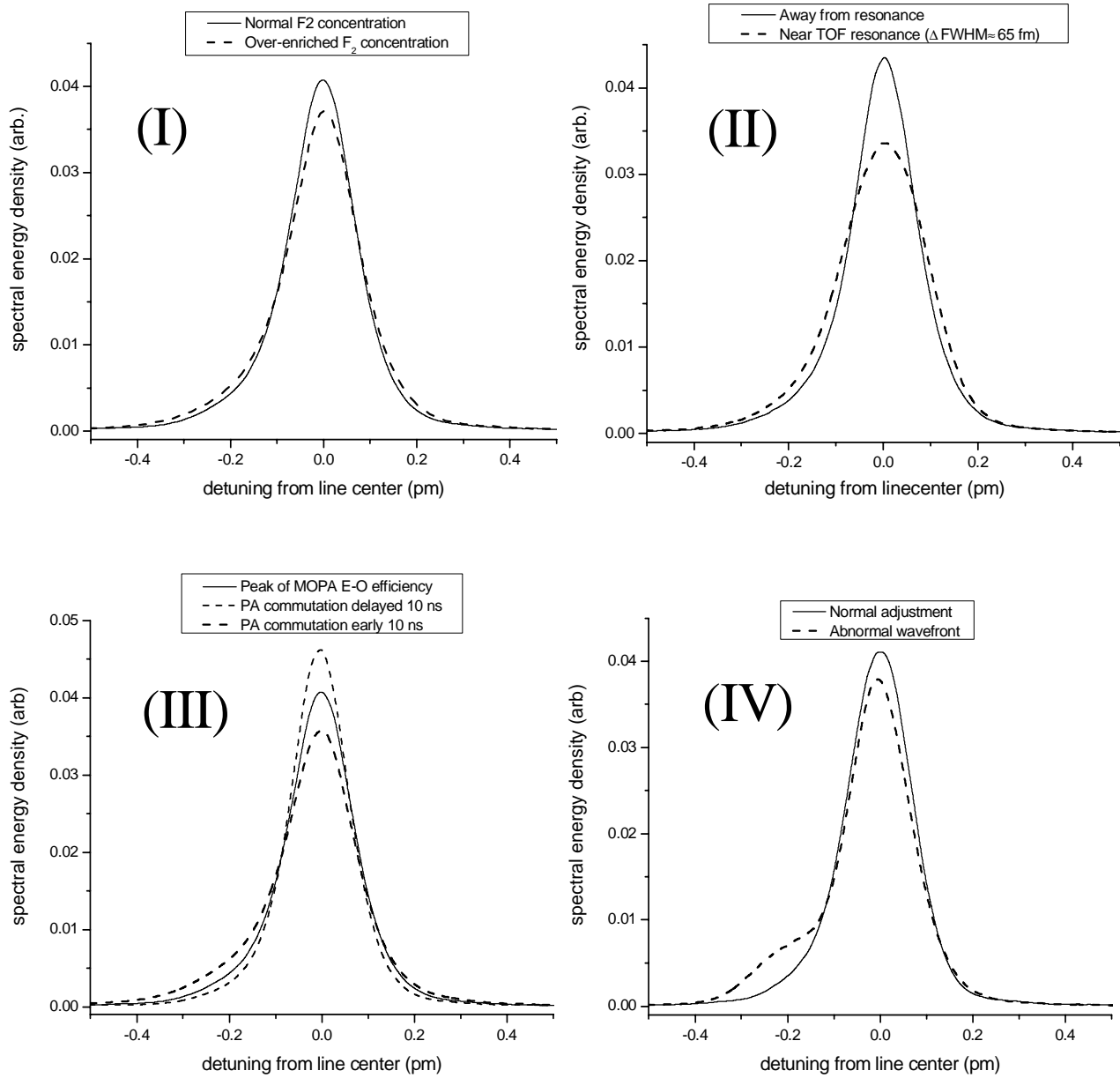


Figure 1. Varieties of spectral shapes, all normalized to unit energy content in a 15 pm inspection interval.

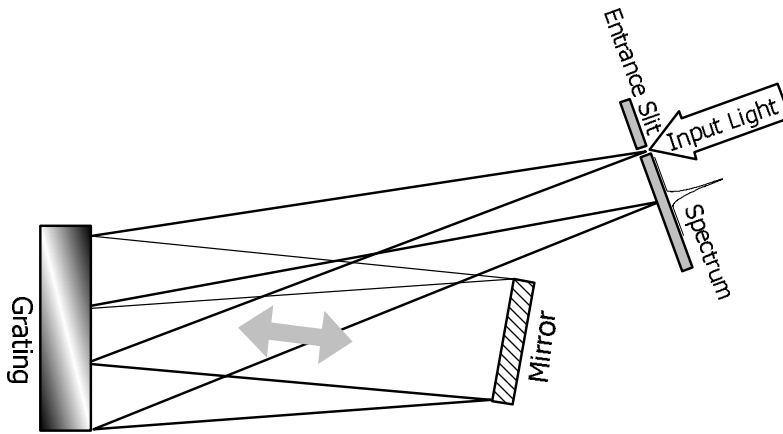


Figure 2. One embodiment of a double-pass grating spectrometer.

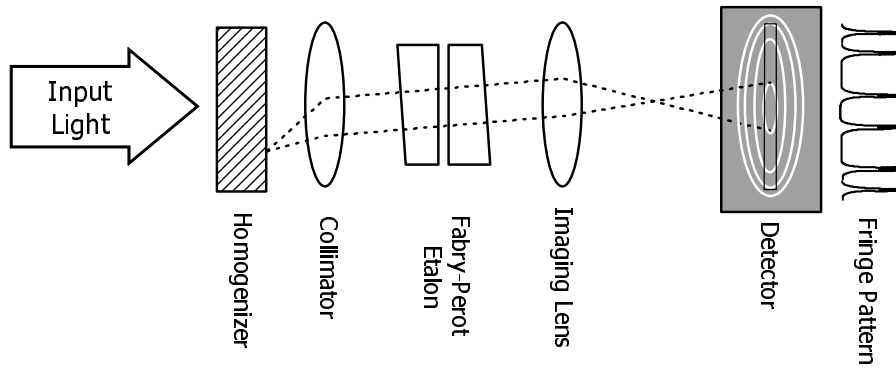


Figure 3. A spectrometer utilizing the angular dispersion of a plane-etalon.

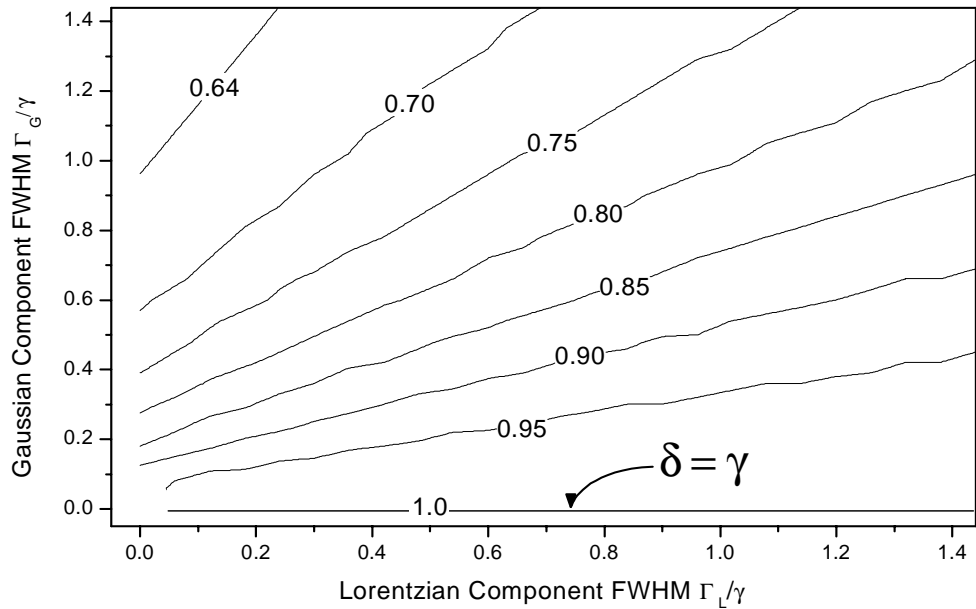


Figure 4. Contours of the difference between Voigt source and Lorentzian instrument-convolved spectral FWHM bandwidth versus shape parameters in units of the instrumental FWHM bandpass γ (see text for details).

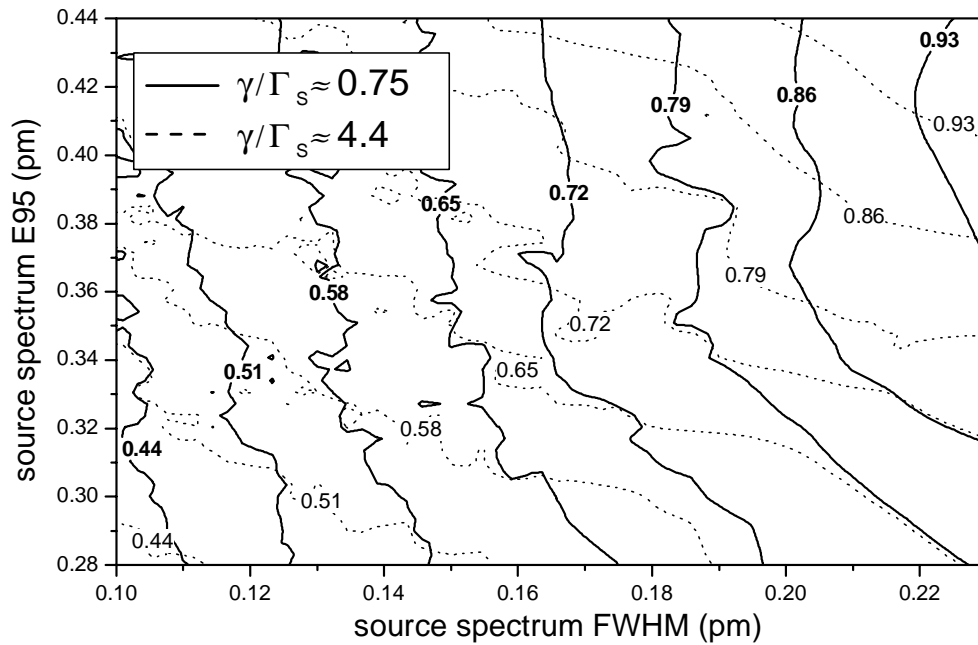


Figure 5. Simulated etalon-spectrometer FWHM fringe contours for ~5000 experimental light source spectra. Two sets are of data shown illustrating the effect of different choices of the etalon FWHM bandpass γ .

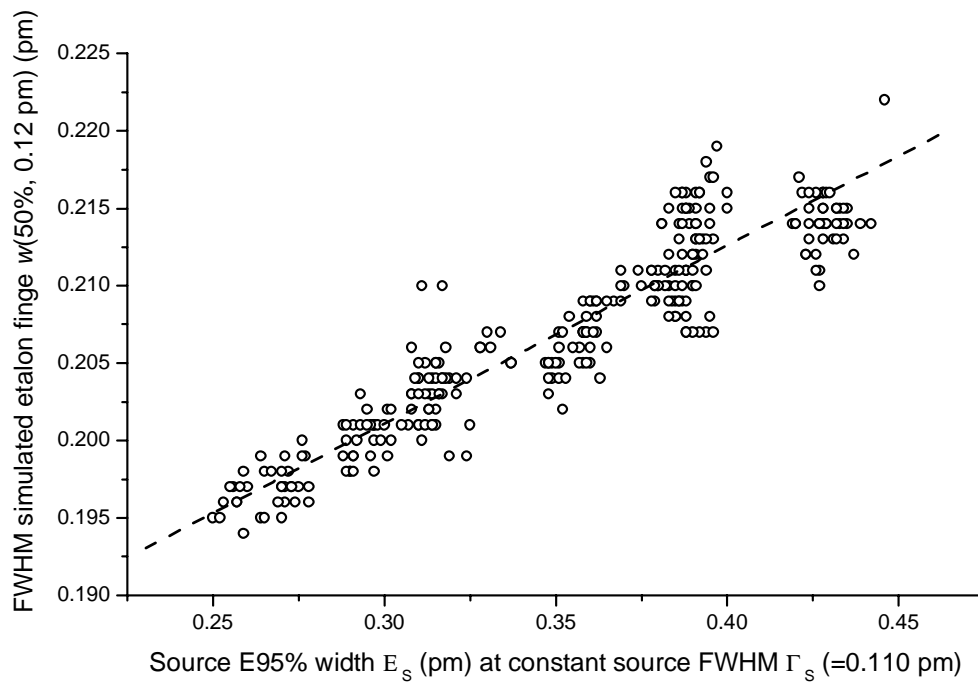


Figure 6. Leakage of energy from the near spectral wings broadens the FWHM of an etalon fringe. A simulation of a Lorentzian spectrometer with 0.12 pm FWHM bandpass convolved with real light source spectra all having identical FWHM bandwidths of 0.11 pm. Clustering of data arises from groups of runs under different operating conditions.

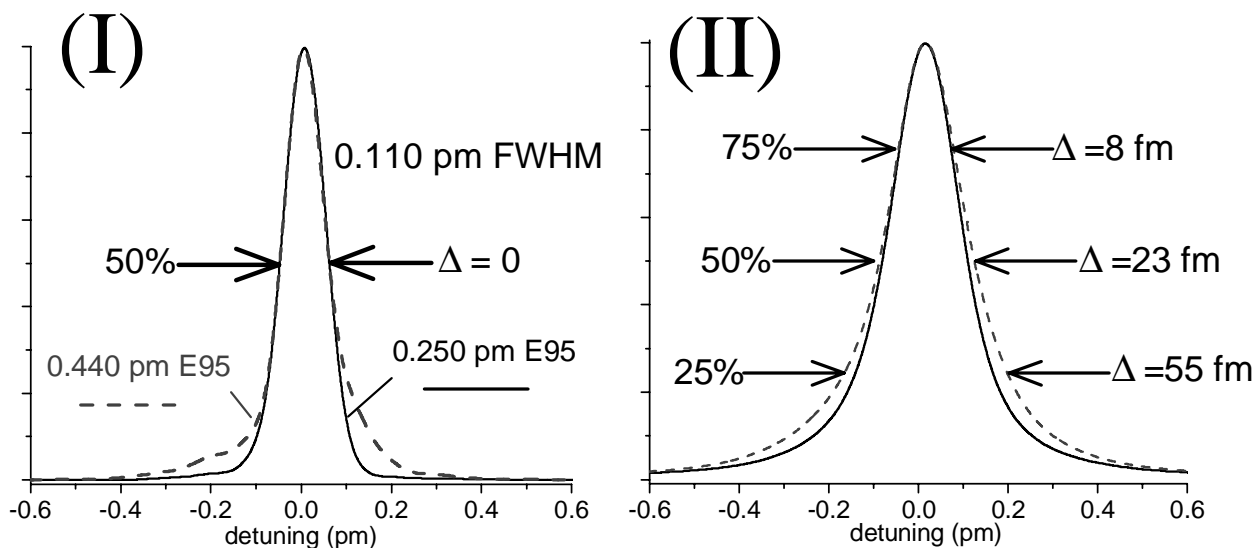


Figure 7. Two measured laser spectra with identical 0.11 pm FWHMs and different E95 bandwidths (I) and their convolutions with a Lorentzian instrument function of 0.12 pm FWHM bandwidth (II). The convolved fringe widths at various thresholds are different for the two spectra; the amount of discrepancy is shown as Δ in (II). This difference is the source of systematic error for constant-offset and point-slope FWHM models due to spectral shape variation, as described in the text.

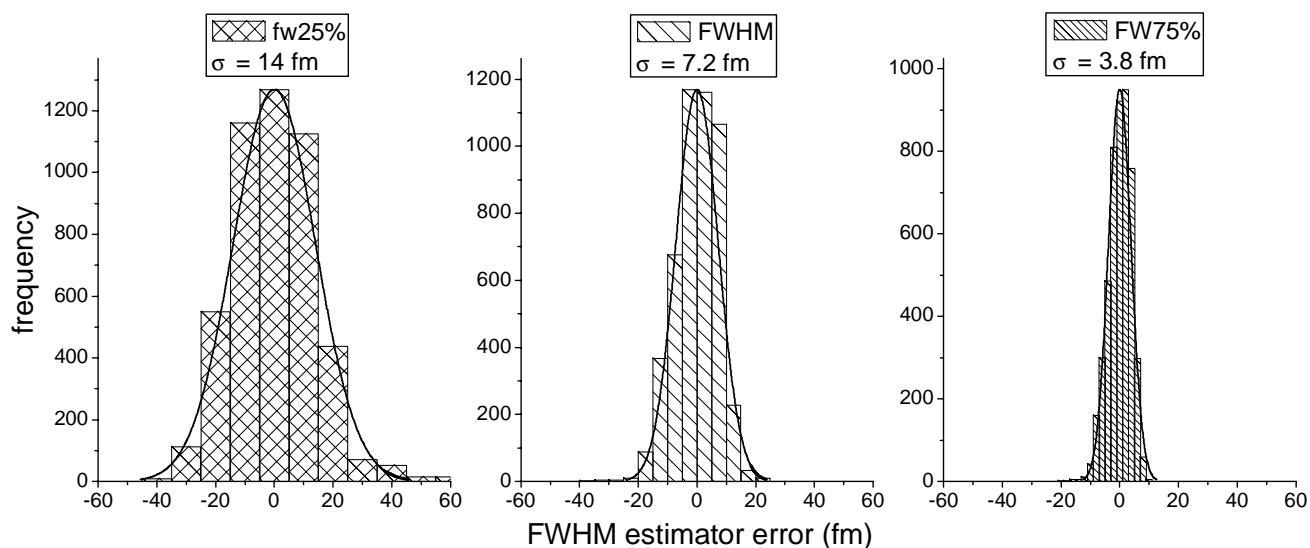


Figure 8. Improvement of point-slope FWHM estimator model performance with fringe width measurement at increasing intensity thresholds $X\%=25\%, 50\%, 75\%$. (Etalon simulation with population of ~ 5000 deconvolved grating spectrometer measured spectra identical to those used in Fig. 5.)

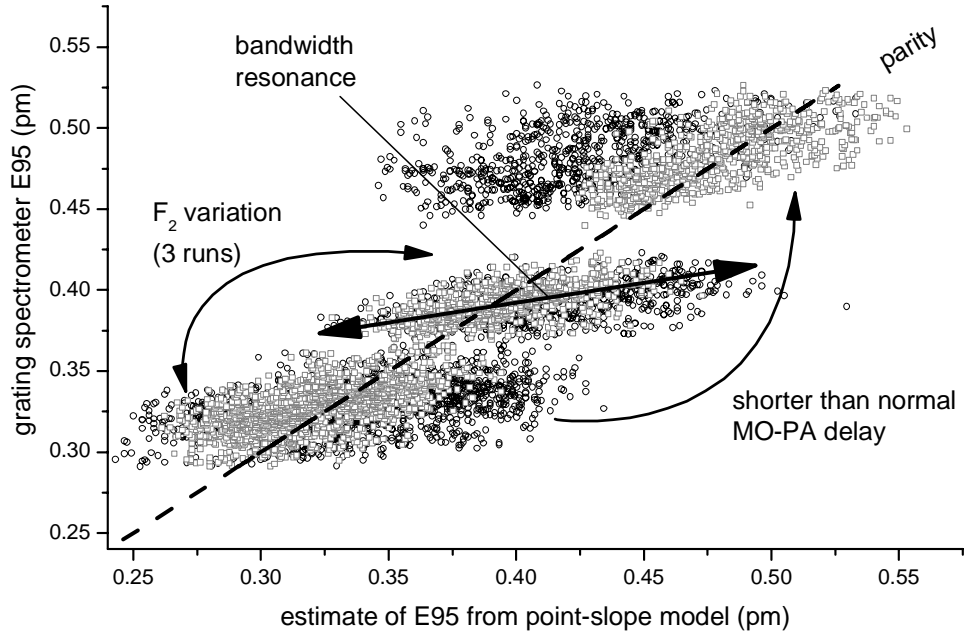


Figure 9. Results of experiments illustrating systematic sensitivity of fringe point-slope model estimation of E95 to spectral shape variation induced by changes in laser operating conditions; 3130 spectra and etalon fringe patterns measured. Grey squares used fringe FW35% as input, black circles used fringe FW75%. Two or three distinct slopes and four distinct intercepts are apparent, corresponding to different spectral-shape subsets of the data.

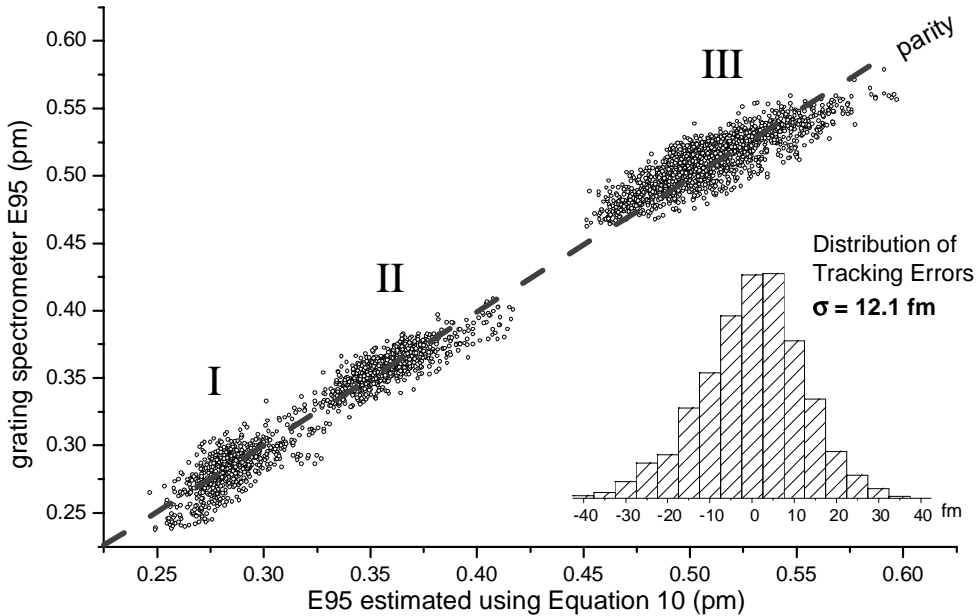


Figure 10. Estimation of E95 using the two intensity-threshold (FW35%+75%) model of Equation 10. 3250 spectra and fringe patterns from 4 separate experiments combined: Group I, normal F_2 concentration with delayed MOPA timing; Group II, normal F_2 and normal timing; Group III, enriched F_2 , also normal F_2 with shortened MOPA timing. Deviation from parity was better controlled compared to point-slope model of Figure 9. The inset shows the distribution of tracking errors for the spectral population, with a sigma of 12.1 fm. About 4 fm of this can be explained by the finite SNR of the source spectrum in the grating spectrometer measurement.